Results in Chemistry 11 (2024) 101766

Contents lists available at ScienceDirect

Results in Chemistry

journal homepage: www.sciencedirect.com/journal/results-in-chemistry

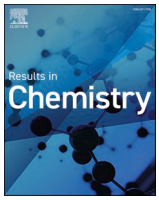

Hybrid virtual screening and molecular dynamics approach for identification of allosteric modulator of EAAT2

Chennu Manisha [a], Nagarjuna Palathoti [b], Jagdish Chand [b], Akey Krishna Swaroop [b], Jubie Selvaraj [b], B.R. Prashantha Kumar [c], Prisil Naveentha X [d], Brindha Durairaj [e], Antony Justin [a,*]

[a] Department of Pharmacology, JSS College of Pharmacy, JSS Academy of Higher Education & Research, Ooty, Nilgiris 643 001, Tamil Nadu, India
[b] Department of Pharmaceutical Chemistry, JSS College of Pharmacy, JSS Academy of Higher Education & Research, Ooty, Nilgiris 643 001, Tamil Nadu, India
[c] Department of Pharmaceutical Chemistry, JSS College of Pharmacy, JSS Academy of Higher Education & Research, Mysuru, 570 015, Karnataka, India
[d] Department of Chemistry, PSG College of Arts & Science, Coimbatore 641 014, Tamil Nadu, India
[e] Department of Biochemistry, PSG College of Arts & Science, Coimbatore 641 014, Tamil Nadu, India

ARTICLE INFO

Keywords:
EAAT2
AK-968/15360623
Virtual screening
Molecular dynamics
Alzheimer's disease

ABSTRACT

EAAT2, a glial protein that clears excess glutamate from synapses, regulates synaptic transmission, and prevents excitotoxicity in neurons is impaired by Aβ induced oxidative stress in neurodegenerative diseases like Alzheimer's disease. Therefore, compounds that enhance EAAT2 function by reducing oxidative stress and excitotoxicity might be neuroprotective. The current study aimed to identify allosteric activators targeting EAAT2 in the treatment of AD using *in-silico*. Virtual screening identified promising candidates from the specs database and demonstrated excellent binding affinity with the allosteric pocket of EAAT2. ADMET studies determined the lipophilicity of the compounds and displayed good permeability across the BBB. MM-GBSA analysis further showed higher binding free energy for two compounds. Subsequently, molecular dynamics simulations confirmed the stability of the complex and its binding ability to the allosteric pocket of EAAT2. These findings identified the compound AK-968/15360623 as a promising lead molecule that could enhance EAAT2 function and prevent neurodegeneration in AD.

1. Introduction

Glutamate is the most abundant excitatory neurotransmitter in the central nervous system (CNS) and is essential for maintaining synaptic transmission [1]. However, excessive glutamate stimulation of postsynaptic receptors via neurons results in excitotoxicity and neuronal death. Therefore, the removal of glutamate from the synapse is required for neuronal survival, and this can be accomplished by the uptake of released glutamate by astrocytic transporters [2,3]. Currently, five structurally distinct subtypes of EAATs have been identified, one of which is excitatory amino acid transporter 2 (EAAT2), which is essential for maintaining glutamate homeostasis and preventing excitotoxicity [1,4]. EAAT2 is highly expressed in astrocytes and contributes to 95 % of glutamate transport activity.

Several neurodegenerative conditions, including cerebral ischemia [5–7], amyotrophic lateral sclerosis (ALS) [8], and Alzheimer's disease (AD) [9], have been linked to glutamate-mediated excitotoxicity mechanisms. Patients with AD have excitotoxic damage to glutamatergic neurons in the cortex and hippocampus [10,11]. Numerous studies have shown that the function of EAAT2 is significantly reduced or damaged in AD due to oxy-radicals and cytokines [9,12–14]. The abnormal deposition of amyloid beta (Aβ) is AD's most prominent pathological feature [15]. Moreover, AD mutants (Amyloid precursor protein/presenilin-1) lacking the EAAT2 protein exhibited cognitive deficits at a younger age [16]. These findings suggested that the dysfunction of EAAT2 is involved in early pathogenic processes in AD that result from the dysregulation of glutamatergic neurotransmission by Aβ and contribute to synaptic dysfunction and cognitive impairment [17].

Parawixin 1 is one of the novel neuroprotective components identified in spider venom that modulates glutamate transport. Parawixin 1 increases glutamate uptake in rat synaptosomes by acting directly and

* Corresponding author.
E-mail address: justin@jssuni.edu.in (A. Justin).

https://doi.org/10.1016/j.rechem.2024.101766
Received 4 May 2024; Accepted 30 August 2024
Available online 31 August 2024

Table 1
Description of binding sites of EAAT2.

Binding site	Site score	Size	D score	Volume (Å)
Site 3	1.02	185	1.18	131.02
Site 5	0.96	131	1.13	71.00
Site 1	0.95	2070	1.07	1415.56
Site 4	0.94	154	1.11	79.57
Site 2	0.93	1125	1.06	661.64

selectively on the EAAT2 glutamate transporter [18,19]. In addition to diverse pharmacological profiles, exogenous neuroprotective activators of EAAT2 such as riluzole [20,21], guanosine [22,23], nicergoline [24,25], [*R*]-[−]-5-methyl-1-nicotinoyl-2-pyrazoline (MS-153) [26], and parawixin-1 produced nonspecific side effects, therefore restricting their use [27]. Additionally, a mutagenesis study revealed that the EAAT2 transporter's structural region, which is made up of the transmembrane (TM) domains 2, 5, and 8, is essential for improving EAAT2 transporter activity [28]. This allowed for the identification of novel allosteric modulators of EAAT2 using hybrid structure-based virtual screening of a vast library of molecules [29]. *In vitro* studies have shown that the allosteric modulator 3-[(4-Cyclohexyl-1-piperazinyl) [1-(2-phenylethyl)-1H-tetrazol-5-yl]methyl]-6-methoxy-2(1H)-quinolinone (GT949) increased EAAT2 activity in primary neuronal-glial culture.

In addition, they have been found to protect neurons from glutamate-mediated excitotoxicity in neuronal-glial cultures. However, GT949 has some limitations for allosteric activation of EAAT2, as it has been shown to be ineffective in halting neurodegeneration caused by oxidative stress because it did not protect neurons in an *in vitro* model of oxidative damage caused by hydrogen peroxide [30]. This could be because reactive stress has damaged the glutamate transporters. Additionally. It has also been shown that GT949 has a high risk of human ether-a-go-go-related gene (HERG) inhibition and poor oral absorption, impacting its cardiac toxicity, bioavailability, and pharmacokinetics. Furthermore, extensive research is required in *in vivo* to evaluate the safety and effectiveness of GT949 in activating the EAAT2 protein. Therefore, the identification of potential positive allosteric activators targeting the EAAT2 transporter is required to prevent Aβ-mediated oxidative damage and excitotoxicity and offers a novel approach in AD.

In the current study, we employed an *in-silico* virtual screening approach to identify potential small molecules capable of functioning as positive allosteric modulators targeting the EAAT2 protein. To accomplish this, a synthesized chemical library was obtained from the specs database and subjected to an initial screening process. Subsequently, the compounds that successfully passed this preliminary screening were further examined through molecular docking simulations to ascertain their interaction with the allosteric binding pocket of EAAT2. In addition, an ADMET analysis was performed to identify candidate compounds exhibiting promising pharmacological characteristics. Thereafter, Molecular Mechanics/Generalized Born Surface Area (MM-GBSA) determined the compounds' binding free energy. Finally, molecular dynamics (MD) simulations were employed to assess the stability of the complexes formed between EAAT2 and individual drugs.

The Schrödinger suite 2021–4 was chosen for these simulations due to its comprehensive and integrated platform with advanced algorithms and state-of-the-art force fields over other software packages. This force field provides predictions of molecular interactions and properties, enhancing the accuracy of our computational results. In our study, we used the OPLS4 force field for water, which is known for its precision in modeling molecular interactions and predicting binding affinities, making it a valuable tool for drug discovery and molecular modeling [31].

In our study, the compound AK-968/15360623 exhibited a favourable binding affinity for EAAT2, and acceptable blood–brain barrier permeability. Consequently, our study suggested that this compound could act as an potential allosteric activator of EAAT2, which may have beneficial effects for neurodegenerative conditions like AD.

2. Materials and methods

2.1. EAAT2 protein preparation

The crystal structure of EAAT2 (PDB ID: 7VR8) was obtained from the RCSB protein data bank (https://www.rcsb.org) [32]. The structure was prepared using Maestro's protein preparation wizard tool (Schrödinger suite 2021–4), which involved the removal of unnecessary water molecules, the addition of missing hydrogen atoms, and the assignment of bond orders. A restrained minimization process was performed using the OPLS4 force field to optimize the protein structure [31].

2.2. Preparation of compound database

A library of 5,00,000 synthetic compounds was downloaded from the Specs database (https://www.specs.net). The compounds were processed using Maestro's builder panel to generate their three-dimensional structures. Subsequently, the LigPrep wizard in Schrödinger software was employed to optimize the compounds, considering different stereoisomers, tautomers, and ionization states at pH 7 ± 2. The optimization utilized the OPLS4 force field, resulting in the generation of optimized structures for further analysis [31].

2.3. Binding pocket prediction

From the reported literature [29], the amino acids His71-Trp472 considered as the allosteric region residues. By utilising the siteMap module in Schrödinger [33] different catalytic pockets were generated in the allosteric region (7VR8.pdb). This analysis involved in examining the entire allosteric region to identify and rank possible binding sites based on various numerical descriptors, including size, degree of enclosure or exposure, tightness, hydrophobic or hydrophilic character, and hydrogen bonding possibilities. The potential binding sites were then prioritized using a weighted average of these values, with the site score serving as the scoring function to evaluate the likelihood of ligand binding and identify pharmaceutically significant binding sites.

2.4. Molecular docking simulation

The virtual screening of synthetic compounds from the specs database (https://www.specs.net) was performed via the predicted binding pocket using the Glide module [34]. Firstly, the compounds were screened using the predicted allosteric binding site and further sequenced by Glide Score (G_{score}) using HTVS. Subsequently, precise screening was employed using standard precision (SP) docking. Then, the compounds with the highest docking scores from SP docking, indicating strong binding affinity and favorable pose quality, were prioritized for extra precision (XP) docking. This selection ensured that only the most promising candidates were subjected to the more detailed and computationally intensive XP docking process [35]. Further, based on the glide score function, the glide energy, and the glide emodel energy, the best-docked structures and the docked poses with the highest negative energy were chosen for further study.

ADMET prediction

The physicochemical and absorption, distribution, metabolism, excretion, and toxicity (ADMET) properties of the chosen compounds were predicted using the QikProp module [36] in Maestro (Schrödinger 2021–4). The pharmacokinetic parameters and toxicological properties, including ADMET, were analyzed for molecular weight, blood–brain barrier (BBB) permeability, hydrophobicity, CNS activity, log P, and log HERG. The molecular pharmacokinetic prediction is useful in lead

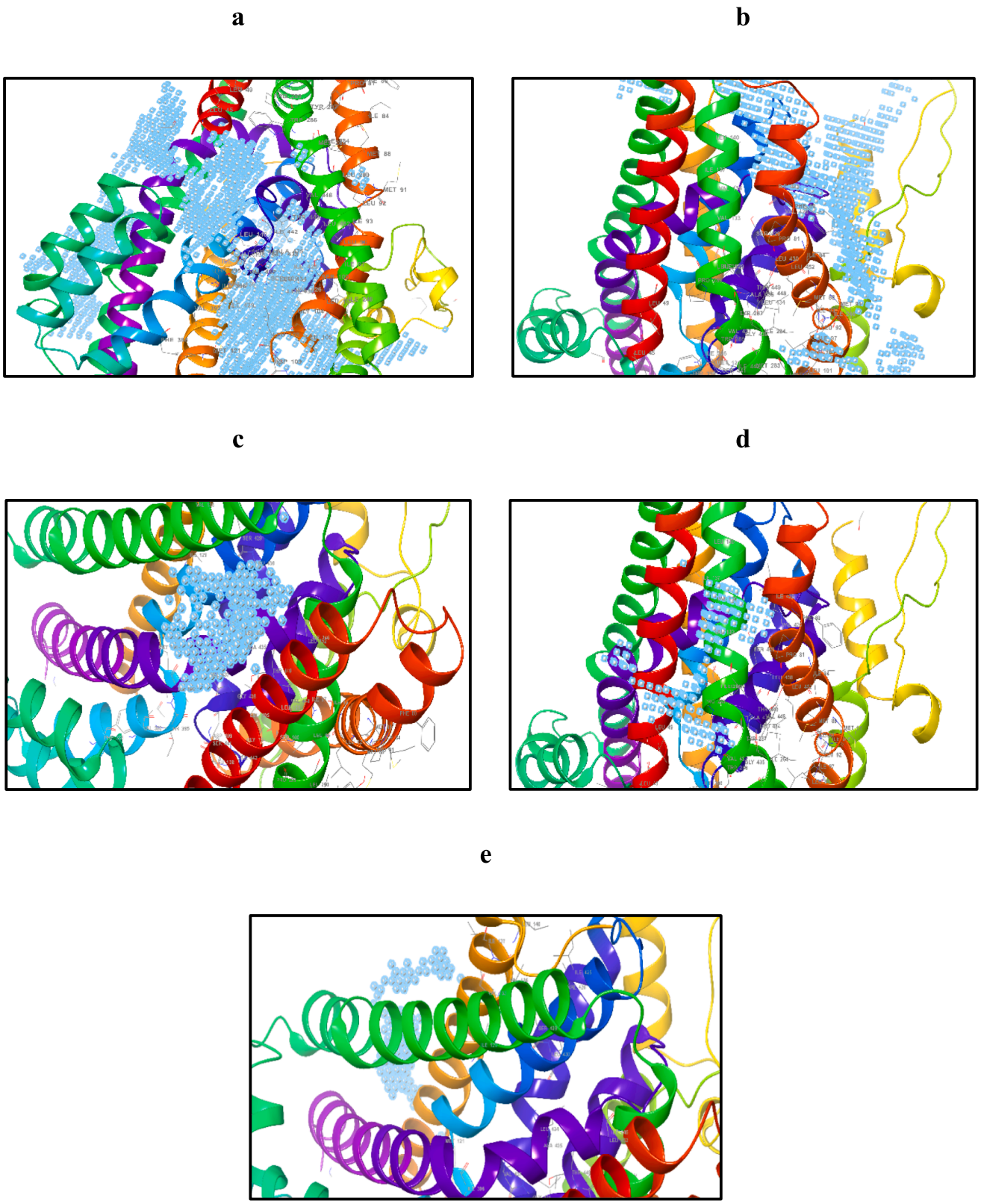

Fig. 1. Predicted druggable pockets by siteMap. **(a)** Site 1, **(b)** Site 2, **(c)** Site 3, **(d)** Site 4, and **(e)** Site 5. The helical structure represents the EAAT2 protein, and the light blue colour spots represent the binding pocket.

optimization and for the development of novel molecules that are druggable. Lipinski's rule of five defined the molecule's rational drug design and discovery [37].

2.5. Binding free energy calculation using Prime/MM-GBSA approach

The top 8 compounds that followed ADMET properties were further selected for MM-GBSA using the Prime module of Schrödinger Suite

Table 2
Extra precision docking score of the top 20 molecules.

No.	Specs ID	[a]G_{score}	[b]G_{emodel}	[c]G_{energy}	[d]ΔG_{Coul}	[e]ΔG_{vdW}
1	AN-648/15101138	−9.40	−96.12	−60.27	−5.48	−54.79
2	AA-504/07472044	−9.09	−78.88	−53.88	−5.69	−48.18
3	AP-845/41779983	−8.73	−78.66	−55.25	−3.38	−51.87
4	AK-778/43413629	−8.70	−69.07	−47.08	−4.82	−42.25
5	AN-652/14870006	−8.55	−89.99	−61.30	−7.54	−53.75
6	AK-968/41017196	−8.38	−75.25	−49.03	−3.05	−45.98
7	AK-968/15363543	−7.67	−76.64	−52.79	−4.07	−48.71
8	AG-690/40756319	−6.99	−93.94	−61.57	−3.28	−58.29
9	AK-968/41024200	−6.70	−80.21	−55.39	−4.43	−50.95
10	AG-205/13184070	−6.80	−79.54	−53.30	−4.37	−48.93
11	AK-968/15363543	−6.62	−82.07	−52.30	−1.26	−51.04
12	AK-968/15360276	−6.56	−71.49	−56.96	−3.16	−53.80
13	AM-900/40673850	−6.42	−83.85	−60.01	−4.62	−55.39
14	AK-968/15360623	−6.39	−68.15	−57.13	−3.28	−53.85
15	AK-968/15252716	−6.26	−104.00	−65.53	−5.25	−60.28
16	AP-501/43059400	−6.21	−79.28	−51.57	−2.88	−48.68
17	AG-690/36164031	−5.41	−117.38	−79.06	−8.54	−70.51
18	AH-487/41187857	−5.25	−109.08	−70.90	−9.16	−61.73
19	AP-970/42895825	−4.96	−65.21	−49.16	−4.97	−44.19
20	AE-848/41827603	−2.25	−73.02	−54.64	−6.48	−48.15
21	Standard (GT949)	−4.28	−68.62	−49.34	−4.78	−44.55

[a] Glide score,
[b] Glide model energy,
[c] Glide energy,
[d] Coulomb energy,
[e] Van der Waals energy.

2021–4 [38]. The complex's binding free energy was calculated using the MM-GBSA approach [39]. Polar solvation was performed using the variable-dielectric generalized Born (VSGB) solvation model [40] and energy calculations were performed using the OPLS force field [31].

2.6. Molecular dynamic simulation

The best-docked pose of the AK-968/15360623/EAAT2 complex was subjected to a 200 ns molecular dynamics simulation using the Desmond module of Schrödinger 2021–4 [41] employing the OPLS4 [31] force field for accurate representation of intermolecular interactions. The system was solvated using the TIP4P [42] water model, which includes explicit water molecules to maintain a realistic solvation environment. The system was prepared by solvating the molecular system in a water box with a buffer distance of 10 Å from the protein atoms. 0.15 M Sodium chloride (NaCl) solutions were added to simulate the physiological environment, and counterions were introduced to neutralize the charge. The system was then minimized, equilibrated, and subjected to a 200 ns MD simulation in an NPT ensemble at a temperature of 300 K and a pressure of 1 atm. Trajectory data was collected every 1.2 ps for coordinate information and every 100 ps for energy. The resulting trajectory was analyzed using Maestro's graphical interface, and an average structure from the final 250 ps of the simulation was refined through energy minimization. The convergence criteria for energy minimization were set at 0.001 kJ/mol/Å.

3. Results

3.1. Identification of catalytic pocket

Based on the results of the siteMap analysis (Table 1), although site 3 had the highest site score of 1.02 among the evaluated binding sites, we ultimately selected site 1 as our target based on important criteria. Site 1 had the highest site score of 0.95, indicating its propensity for ligand binding. In terms of size, site 1 had a substantial size of 2070 units, suggesting a spacious binding pocket for potential interactions. The D score for site 1 was 1.07, indicating a high degree of enclosure and the potential for favorable ligand interactions. Additionally, site 1 exhibited a significant volume of 1415.56 Å (Fig. 1a), further supporting its suitability as a target for ligand binding. Despite site 3 having a marginally higher site score (Fig. 1c), the combined attributes of site 1 made it a more promising candidate for further exploration as a potential binding site that can interact with EAAT2 and serve as allosteric modulators (Fig. 1).

3.2. Virtual screening and binding energy evaluation

In our study, we performed virtual screening and evaluated the binding free energy of a library of synthetic compound databases obtained from specs. Our goal was to identify potential allosteric activators targeting a specific binding site, referred to as allosteric binding site 1. To begin, we subjected a total of 5,00,000 compounds to HTVS. Through this initial screening, we were able to filter down to a subset of 1,317 compounds using SP docking, which helped us prioritize the most promising candidates. Next, we performed the extra-precision docking results, which provide valuable insights into the binding affinities and energies of the 20 selected synthetic compounds. These compounds were carefully chosen based on their XP glide score (G_{score}), with a defined cut-off score of −9.40 kcal/mol, indicating strong binding potentials as allosteric activators compared to standard GT949, which has a low G_{score} of −4.28 kcal/mol.

A range of G_{score} for the compounds has been observed, varying from −9.40 to −2.25. The G_{score} represents the global score, reflecting the overall binding affinity of a compound to the target site. Higher negative G_{scores} indicated stronger binding interactions. Upon examining the glide model energy (G_{emodel}) values, it has been observed that they range from −117.38 to −65.21. More negative G_{emodel} values indicate more favorable binding energies. Moving on to glide energy (G_{energy}), the values span from −79.06 to −47.08. More negative G_{energy} values indicate stronger coulombic attractions between the compound and the target site. Additionally, we consider the coulomb energy (ΔG_{Coul}) and Van der Waals energy (ΔG_{vdW}) values. The ΔG_{Coul} values range from −9.16 to −1.26, while the ΔG_{vdW} values range from −70.51 to −42.25. More negative values for both parameters suggest stronger interactions and favorable binding energies (Table 2). Overall, virtual screening successfully identified a set of 20 synthetic compounds that hold promise as allosteric activators targeting allosteric binding site 1 of the EAAT2 protein. These compounds demonstrated favorable binding energies and were selected based on their high affinity for the target site compared to standard GT949. Further, all 20 compounds and standard GT949 were subjected to ADMET evaluation to predict their pharmacological and toxicological properties.

3.3. ADMET properties

The ADMET data for the top 20 compounds and standard GT949 gives us insight into their characteristics and applicability to our investigation. The molecular weight ranged from 420.89 to 820.94 g/mol, indicating a diverse set of compound sizes. Hydrogen bonding capacity and lipophilicity, crucial for drug-receptor interactions, varied across the compounds, as denoted by the number of hydrogen bond donors and acceptors. Lipophilicity, as measured by QPlogPo/w, ranged from 4.58 to 9.00, signifying differences in hydrophobicity. Caco-2 permeability values (QPPCaco) ranged from 28.79 to 2632.72 nm/sec, reflecting diverse potentials for intestinal absorption. Higher permeability suggests a greater likelihood of oral absorption, except for a few compounds. CNS activity varied, indicating differences in the ability of compounds to penetrate the blood–brain barrier and affect the CNS. Also, the solvent-accessible surface area (SASA) of the compounds was found to be between 713.61 and 1331 $Å^2$, which shows that these molecules fit well in the binding pocket. Polar surface area (PSA), ranging from 75.90 to 187.09 Å, provided insights into molecular size and surface exposure, influencing compound solubility and interactions with targets.

Furthermore, HERG inhibition (QPlogHERG) values ranged from

Table 3
ADMET properties of the top 20 compounds.

Specs ID	[a]Mol. Wt	[b]donor HB	[c]accpt HB	[d]Rule of five	[e]% Human oral abspn	[f]CNS	[g]SASA (Å^2)	[h]QPlogPo/w	[i]QPPCaco (nm/sec)	[j]QPlog HERG	[k]PSA	[l]QPlogBB
AN-648/15101138	598.65	2	9.5	2	90.54	−1	956.01	6.34	840.14	−4.90	106.44	−0.807
AA-504/07472044	480.56	2	6.5	1	100	−2	919.98	6.45	1317.20	−8.78	87.40	−1.168
AP-845/41779983	566.52	1	6	2	94.75	−1	874.45	7.17	774.41	−7.93	79.56	−0.828
AK-778/43413629	420.89	1.5	5.75	0	100	−2	713.61	4.58	423.87	−6.81	94.51	−1.255
AN-652/14870006	586.64	0.5	11.5	2	75.78	−2	988.62	5.22	292.47	−8.69	136.89	−1.724
AK-968/41017196	576.55	2	5	2	95.38	−2	906.17	7.33	748.06	−6.99	91.5	−1.033
AK-968/15363543	580.68	1	5	2	100	0	912.98	7.91	1195.26	−6.58	92.12	−0.457
AG-690/40756319	522.62	0.5	6.75	2	79.95	−2	936.92	6.39	208.75	−8.30	119.23	−2.216
AK-968/41024200	525.70	2	5	2	95.33	−2	907.87	7.22	806.41	−7.10	88.46	−1.119
AG-205/13184070	506.60	1	4.25	2	100	0	904.17	8.28	2632.72	−9.54	56.00	−0.475
AK-968/15363543	577.74	2	5.75	2	100	−2	949.29	7.58	845.90	−7.44	92.11	−1.196
AK-968/15360276	654.28	1.25	7.25	2	95.38	0	856.76	6.59	1302.78	−7.13	95.79	−0.057
AM-900/40673850	540.03	1	5.75	2	94.98	−1	859.38	6.87	999.96	−7.83	80.88	−0.86
AK-968/15360623	**575.38**	**1.25**	**7.25**	**2**	**90.52**	**0**	**825.07**	**5.92**	**1153.42**	**−4.21**	**96.80**	**−0.299**
AK-968/15252716	598.70	2	7	2	100	−1	948.57	7.85	1410.07	−9.11	86.60	−0.955
AP-501/43059400	477.94	1	5.5	1	100	0	791.13	6.29	1189.75	−8.11	75.90	−0.575
AG-690/36164031	820.94	2	11	2	79.87	−2	1331	9.00	28.79	−9.55	187.09	−3.649
AH-487/41187857	566.57	2	8.5	3	46.02	−2	945.77	5.01	39.54	−7.85	173.38	−3.071
AP-970/42895825	459.93	1	7	1	100	0	792.60	5.3	1259.73	−7.73	77.07	−0.523
AE-848/41827603	583.02	2	6	2	90.71	−2	873.35	6.97	533.93	−7.63	99.51	−1.016
Standard (GT949)	527.66	1	10.25	1	62.06	1	887.63	3.67	30.36	−8.41	105.80	−0.64
Recommended values	130–725	0–6	2–20	Max 4	> 80 % is high, < 20 % is poor	−2 to + 2	300–1000	−2.0—6.5	> 500 great, < 25 poor	Below −5	7–200	−3—1.2

[a] Mol Wt: Molecular weight,
[b] donorHB: Estimated number of hydrogen bonds that would be donated by the compound,
[c] accptHB: Estimated number of hydrogen bonds that would be accepted by the compound,
[d] Rule of five: Number of violations of Lipinski's rule of five,
[e] Percentage human oral abspn: Human oral absorption,
[f] CNS: Predicted central nervous system activity on a –2 (inactive) to + 2 (active) scale,
[g] SASA: Total solvent accessible surface area,
[h] QPlogPo/w: Predicted octanol/water partition coefficient,
[i] QPPCaco: Predicted apparent Caco-2 cell permeability in nm/sec,
[j] QPlogHERG: Predicted IC_{50} value for blockage of HERG K^+ channels,
[k] PSA: Van der Waals surface area of polar nitrogen and oxygen atoms,
[l] QPlogBB: Predicted brain/blood partition coefficient.

−4.21 to −9.55, indicating the potential to influence the HERG potassium channel and the associated risk of cardiac side effects. The BBB permeability (QPlogBB) value, which ranged from −0.057 to −3.649. This parameter indicates the compounds' ability to penetrate the BBB, with higher values implying an increased likelihood of BBB permeation. Considering these results, compounds AK-968/15360623 and AN-648/15101138 stand out as they exhibit favorable characteristics in multiple aspects compared to standard GT949, which exhibited a high risk of HERG inhibition, moderate oral absorption, and low Caco-2 permeability. The screened compounds demonstrate good lipophilicity, high Caco-2 permeability, and a relatively low risk of HERG inhibition, suggesting their potential as a drug candidate with favorable oral absorption and reduced cardiac toxicity. Additionally, it shows a favorable BBB permeability value, indicating its ability to cross the blood–brain barrier, which is particularly important for therapeutic targets within the CNS (Table 3). Further, out of 20 compounds, 8 compounds from this subset that exhibit appropriate properties of ADMET within the recommended range [43] were subjected to further analysis using MM-GBSA, providing additional information about their binding characteristics.

Table 4
Binding free energy calculation by Prime/MM-GBSA approach of the top-ranked hits in the catalytic pocket of EAAT2 (7VR8.pdb).

No.	Specs ID	[a]ΔG_{Bind}	[b]ΔG_{Coul}	[c]ΔG_{Cov}	[d]ΔG_{HB}	[e]ΔG_{Lipo}	[f]ΔG_{Solv}	[g]ΔG_{vdW}
1	AN-648/15101138	−79.67	10.69	13.42	0.17	−34.17	12.02	−78.21
2	AA-504/07472044	−60.67	5.65	13.9	1.5	−40	25.93	−66.69
3	AK-778/43413629	−31.77	28.21	0.49	3.27	−25.86	−12.13	−30.89
4	AN-652/14870006	−75.75	−17.09	13.5	0.75	−33.85	29.65	−67
5	AG-690/40756319	−79.50	34.35	−7.09	−0.46	−38.1	−9.52	−58.17
6	AK-968/15360623	−82.74	29.12	8.56	0.38	−35.66	7.26	−88.71
7	AP-501/43059400	−78.69	17.52	4.87	−0.48	−37.84	4.43	−64.98
8	AP-970/42895825	−62.7	22.61	3.22	1.73	−27.85	−4.27	−57.74
9	Standard (GT949)	−51.37	4.17	9.65	−1.52	−15.91	10.68	−56.19

[a] Free energy of binding,
[b] Coulomb energy,
[c] Covalent energy (internal energy),
[d] Hydrogen bonding energy,
[e] Hydrophobic energy (non-polar contribution estimated by solvent accessible surface area),
[f] Electrostatic solvation energy,
[g] Van der Waals energy.

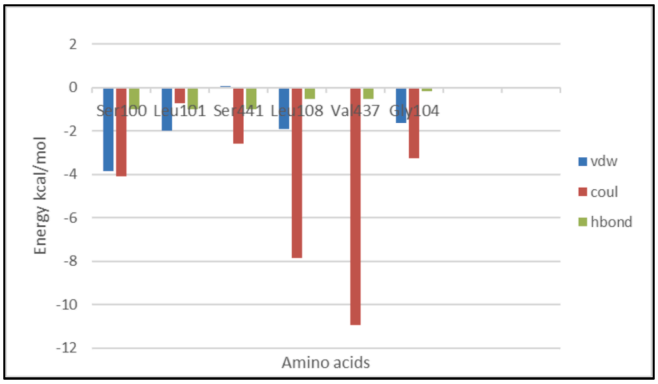

Fig. 2. Graphic illustration of the binding energy of various amino acids within the stable complex AK-968/15360623. The X-axis represents different amino acids, while the Y-axis shows the energy values in kcal/mol. The bars are colour-coded to represent different types of interactions: van der Waals forces (vdw), coulombic (coul) and hydrogen bonding (hbond).

3.4. MM-GBSA

The binding free energy evaluation by MM-GBSA of the top 8 molecules reveals a range of values, indicating their varying binding affinities and interactions with the target site. Among these compounds, the binding free energy values (ΔG_{Bind}) range from −82.74 kcal/mol to −31.77 kcal/mol. Looking at the contributions from specific energy components, the coulomb energy values (ΔG_{Coul}) vary from 34.35 kcal/mol to −17.09 kcal/mol, indicating different levels of coulombic interactions. The covalent energy values (ΔG_{Cov}) span from 13.9 kcal/mol to −7.09 kcal/mol, representing variations in covalent interactions. In terms of hydrogen bonding interactions (ΔG_{HB}), the values range from 3.27 kcal/mol to −0.46 kcal/mol. The lipophilic interactions (ΔG_{Lipo}) show a range from −40 kcal/mol to −25.86 kcal/mol, reflecting the diversity of hydrophobic interactions.

The solvation effects (ΔG_{Solv}) range from 29.65 kcal/mol to −4.27 kcal/mol, indicating differences in the compounds' solvation properties. The contributions from van der Waals interactions (ΔG_{vdW}) vary from −88.71 kcal/mol to −30.89 kcal/mol, representing the strength of these forces in stabilizing the binding complexes. Among these 8 molecules, compounds AK-968/15360623, and AN-648/15101138 stand out as the best candidates due to their highly negative binding free energy values of −82.74 and −79.67 kcal/mol compared to standard GT949 (−51.37 kcal/mol) (Table 4). Compounds AK-968/15360623 and AN-648/15101138 exhibited favorable hydrophobic interactions and demonstrated a higher lipophilic nature. These characteristics suggest that it has a greater affinity for hydrophobic regions within the target protein, which can be advantageous for its binding and modulation of EAAT2 protein activity. The graphic quantification of AK-968/15360623 stable complex with negative binding free energy has been shown in Fig. 2.

The 3D interactions of the top 2 hits and the standard GT949 obtained from MM-GBSA and XP docking scores are shown in Fig. 3. The docked poses of the selected 2 hits and standard GT949 exhibited non-covalent interactions, such as hydrogen bonds and hydrophobic interactions. The bromo pyrazole of ligand AK-968/15360623 formed a halogen interaction with SER441 (Fig. 3a). The amide group of ligands AN-648/15101138 formed hydrogen bond interaction with LEU 108 (Fig. 3b). The carbonyl group in the quinoline ring of ligand GT949 formed hydrogen bond interactions with ALA 445, and the amide group in the quinoline ring formed hydrogen bond interactions with ILE 442 (Fig. 3c). Subsequently, molecular docking studies indicate that ligands interact with different amino acid residues of the EAAT2 protein through non-covalent bonds, such as halogen interactions and hydrogen bonds. Considering the overall importance of higher binding free energy, hydrophobic, lipophilic interactions, and ADMET properties in the context of the desired allosteric activation of EAAT2 protein, compound AK-968/15360623 appears to be a suitable candidate compared to compound AN-648/15101138 and standard GT949. Therefore, compound AK-968/15360623 was chosen as the primary candidate for further investigation in molecular dynamic simulation studies due to its favorable ADMET characteristics and promising binding free energies.

3.5. Molecular dynamic simulation

To assess the stability and convergence of the docked complex between compound AK-968/15360623 and EAAT2, molecular dynamics simulations were conducted for a duration of 200 ns. The simulations revealed that the root mean square deviation (RMSD) of the protein's C-α backbone experienced minor fluctuations of 1.3 to 2.7 Å between 5–25 ns, and then stabilized respectively, in the range of 2.3 to 3 Å from 25-95 ns. Subsequently, the RMSD of the protein exhibited a minor fluctuation of 2.7 to 3.2 Å between 95–100 ns, and then again stabilized in the range of 2.8 to 3.7 Å from 100-200 ns. Importantly, this indicates that the protein structure maintained higher flexibility throughout the simulation trajectory. In contrast, the ligand (compound AK-968/15360623) initially exhibited major fluctuations with an RMSD of 1 to 3.1 Å (2.1 Å) between 5–10 ns. However, it immediately reached a stable state with an RMSD of 1.1 to 3.3 Å (2.2 Å) between 10–200 ns. Lower RMSD values (3 Å) [44] indicates the better stability of the complex. These findings suggest that compound AK-968/15360623 in complex with EAAT2 exhibits acceptable stability (<3 Å) [44] and maintains its

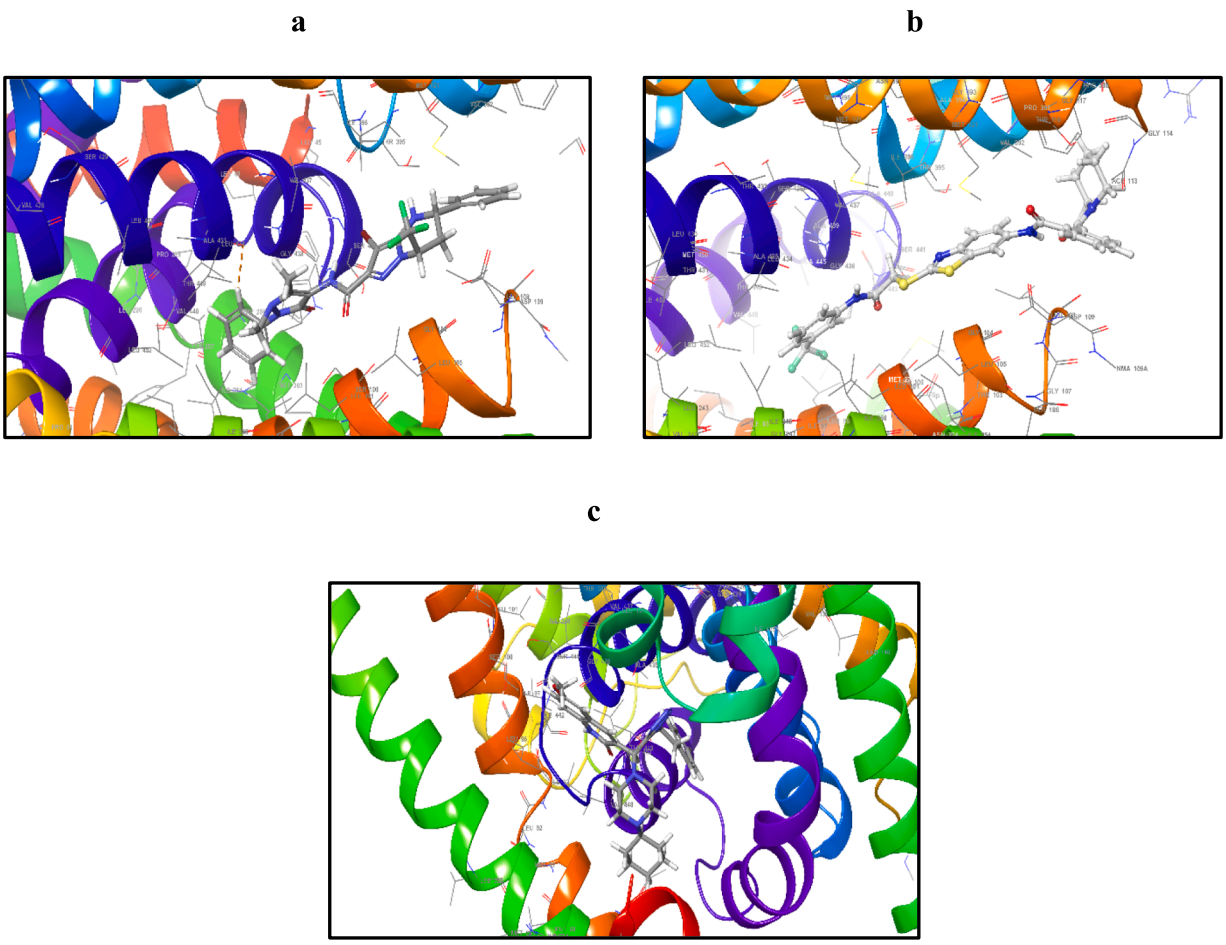

Fig. 3. 3D interaction diagrams of binding poses of compounds within the EAAT2 allosteric binding pocket. **(a)** AK-968/15360623, **(b)** AN-648/15101138, and **(c)** GT949. In the 3D diagrams, the ribbon structures represent the EAAT2 protein, while the stick model shows the compounds and their interactions.

binding pose during the molecular dynamic's simulation, supporting its potential as a promising candidate for further investigation in the context of allosteric activation of EAAT2 protein for glutamate uptake (Fig. 4a).

The flexibility of residues in the ligand binding site was assessed using root mean square fluctuation (RMSF) measurements. The RMSF values indicated moderate fluctuations ranging from 1.6 to 4.2 Å, 0.8 to 5 Å, and 1.0 to 5 Å for different residues, while higher fluctuations were observed ranging from 1.2 to 6.2 Å. Among the residues, ILE 70, NMA 109, NMA 147, SER 163, SER 164, LYS 193, NMA 193, ILE 230, and LYS 231 exhibited the highest RMSF values, indicating greater conformational flexibility in the protein. On the other hand, residues such as HIS71, ASP83, MET86, LEU290, LEU295, GLY298, LYS299, PRO443, SER465, and TRP472, which are part of the allosteric pocket, showed lower RMSF values, suggesting a more stable conformation during the molecular dynamic's simulation (Fig. 4b).

A total of 20 protein–ligand contacts were formed with amino acids of the EAAT2 protein, from ILE 93 to LEU 101, THR 103 to MET 125, ILE 246 to VAL 437, and ALA 440 to LEU 452. From Fig. 5a, it was stated that the ligand is stabilized by forming most of the hydrophobic interactions (1 %–40 % of simulation time) with residues ILE 93, LEU 96, ILE 97, LEU 101, LEU 108, MET 121, MET 125, ILE 246, ILE 396, LEU 434, VAL 437, ALA 440, ILE 442, VAL 448, and LEU 452. Over the course of 1 %–65 % of the simulation trajectory, it also formed hydrogen bonds with SER 100, VAL 437, and SER 441. This complex also formed many water bridges with SER 100, LEU 101, THR 103, LEU 105, ASN 274, and SER 441 up to 1 %-98 % of simulation. Multiple protein–ligand interactions were observed for SER 100, LEU 101, VAL 437, and SER 441. These findings highlight the stability of the ligand within the allosteric binding site of the protein and emphasize the importance of hydrophobic interactions in complex formation. Overall, our study supports the potential of compound AK-968/15360623 as a lead candidate for targeting EAAT2 in neurodegenerative diseases.

We analyzed the 2D-trajectory interaction diagram (Fig. 5b) to gain insights into the binding interactions between the ligand (AK-968/15360623) and the allosteric binding pocket of the EAAT2 protein. We observed a strong hydrogen bond between SER 441 and the amide group of the compound at 60 % occurrence. Furthermore, the carbonyl group in the pyrazole ring formed a water bridge with SER 100 at 40 % of the simulation time. The hydrophobic interactions between the ligand and the EAAT2 protein were observed with the ILE 97 residue, indicating their contribution to the overall stability of the complex. These findings highlight that specific binding interactions and hydrophobic interactions play a crucial role in the ligand's interaction with the EAAT2 protein.

4. Discussion

S. Kortagere *et al.* demonstrated the three-dimensional structure of the EAAT2 protein using homology modeling and subsequent prediction of the allosteric binding pocket *via* molecular dynamic simulation and site-directed mutagenesis [29]. In the current work, the crystallized protein (PDB ID: 7VR8) was used and the allosteric binding site was identified using siteMap analysis. Our investigation utilized; a site 1 allosteric binding pocket that possessed all the amino acid residues necessary for activation of EAAT2.

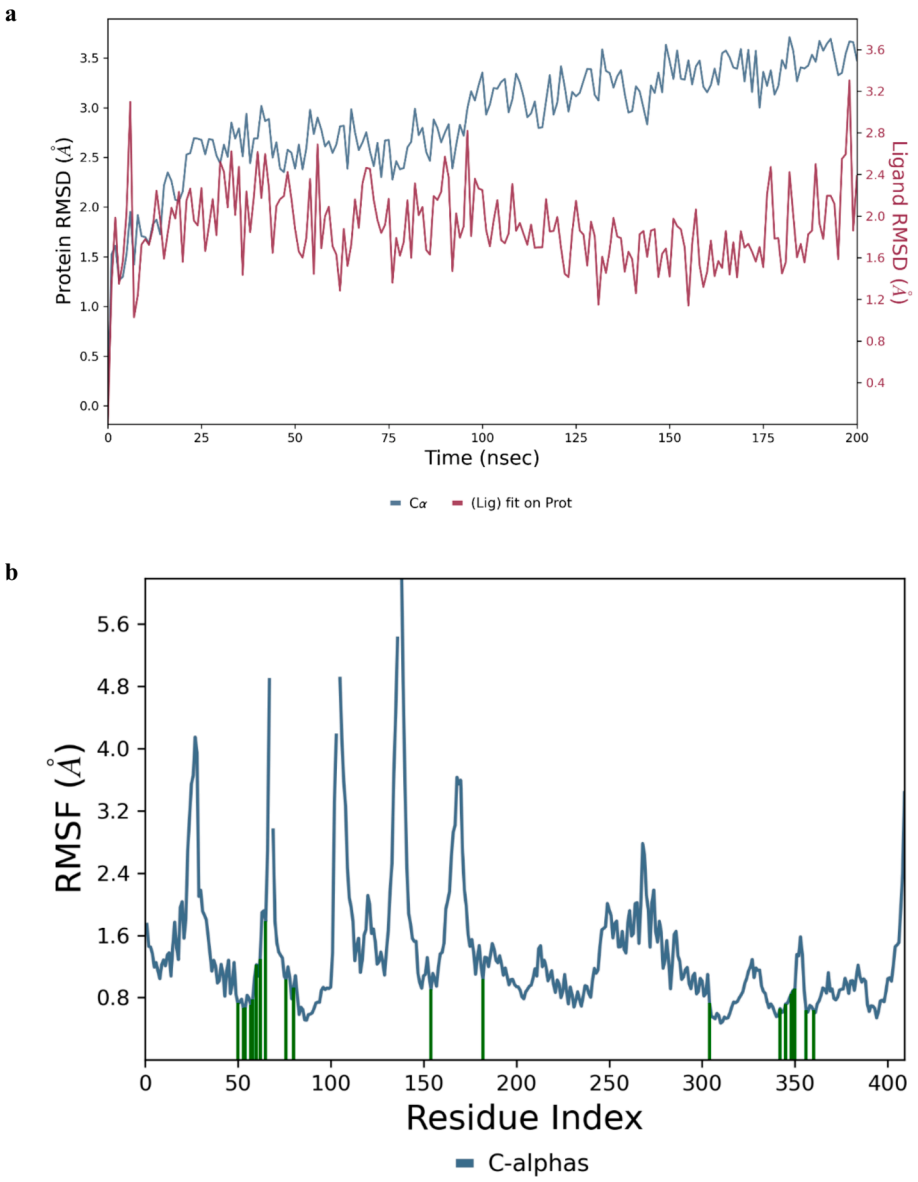

Fig. 4. MD simulations of the complex of compound AK-968/15360623 with EAAT2. **(a)** RMSD and **(b)** RMSF.

Furthermore, a five-point receptor-based pharmacophore model was designed for HTVS and identified GT949 as a positive allosteric modulator of EAAT2. The receptor-based pharmacophore has an aromatic ring, hydrophobic groups, hydrogen bond donor and acceptor groups [29]. In the present study, virtual screening has been performed, evaluating the binding free energy of a library of synthetic compound databases obtained from specs and identifying the compound AK-968/15360623 as an allosteric activator. The compound AK-968/15360623 also possesses two aromatic rings, two hydrogen bond donors, and four hydrogen bond acceptors. Therefore, the presence of similar pharmacophoric features may be the reason for the increased EAAT2 activation.

According to earlier findings, the standard compound GT949 exhibited a high risk of HERG inhibition and moderate oral absorption [30] and additionally, it has limited intestinal absorption based on poor Caco-2 permeability. The present study found that the compound AK-968/15360623 had optimal values for good lipophilicity, BBB permeability, Caco-2 permeability, and a relatively low risk of HERG inhibition, suggesting its potential as a drug candidate with improved oral bioavailability, blood brain barrier permeability, and lower cardiac risk.

Subsequently, relative binding free energies were evaluated using MM-GBSA for GT949, which was not demonstrated in earlier studies. The binding free energy of the compound AK-968/15360623 was found to be higher compared to GT949. Therefore, considering overall results, the compound AK-968/15360623 would be a more promising potential candidate than GT949 for allosteric activation of the EAAT2 protein due to its greater binding free energy, hydrophobic, lipophilic, and ADMET characteristics. A molecular dynamics simulation study of the AK-968/15360623/EAAT2 complex was stable enough in RMSD and subsequently showed lower RMSF values for the residues in the allosteric pocket, including HIS71, ASP83, MET86, LEU290, LEU295, GLY298, LYS299, PRO443, SER465, and TRP472. Moreover, the protein–ligand interaction fraction results in a greater number of hydrophobic interactions that play a crucial role in the overall stability of the complex.

It has been demonstrated that the presence of the five-membered azole rings, such as pyrazole, pyrrole, tetrazole, and imidazole, has antioxidant and anti-inflammatory properties and plays a major role in neuroprotective activities in the context of neurodegenerative disorders. The fact has been substantiated by the chemical structure of the following activators: riluzole has a benz thiazole moiety [20,21], nicergoline has a pyrrole moiety [24,25], guanosine has a purine moiety [22,23], MS-153 has a tetrazole moiety [26], and the direct allosteric

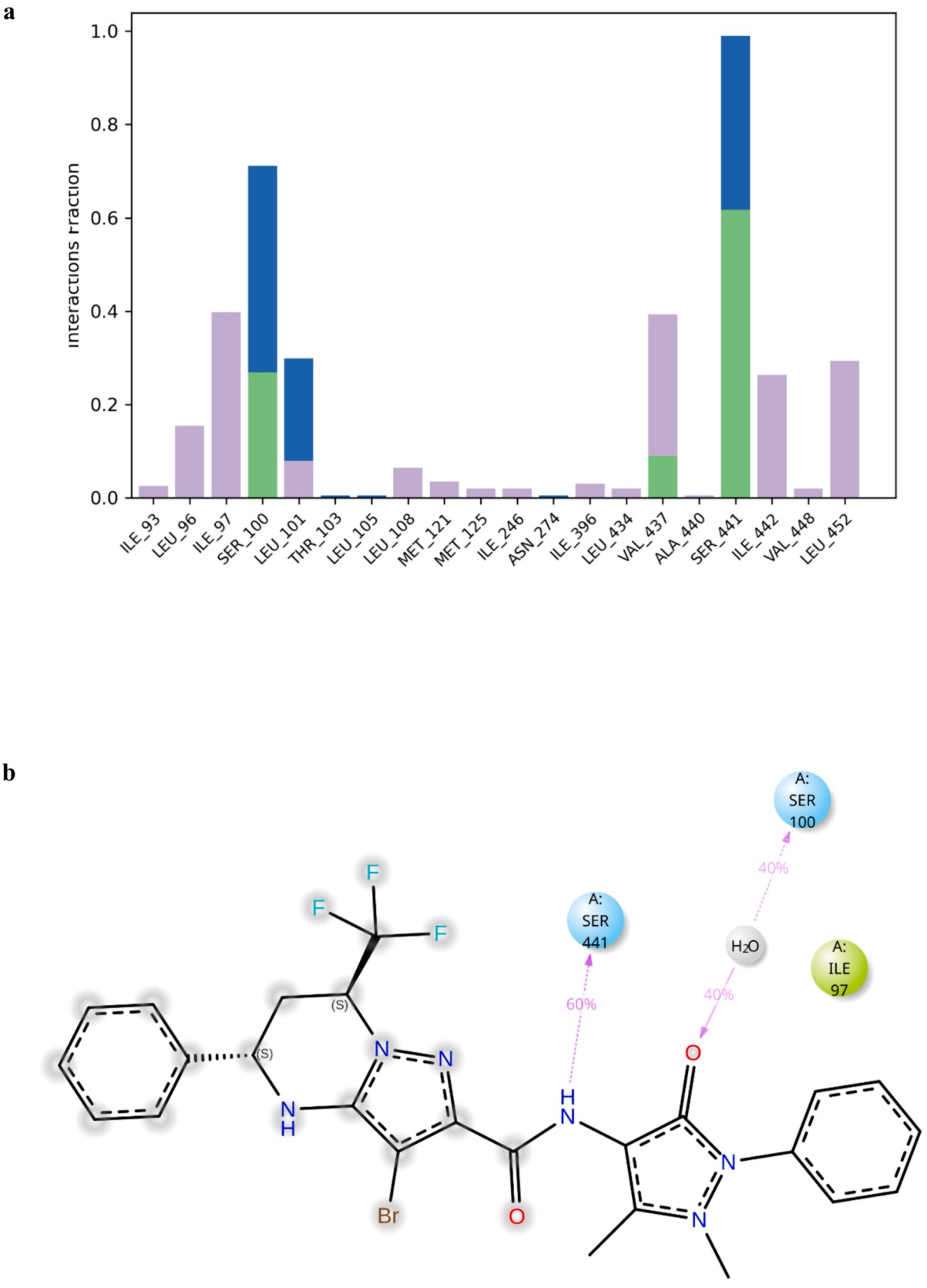

Fig. 5. MD simulations of the complex of compound AK-968/15360623 with EAAT2. **(a)** Interaction fraction, and **(b)** 2D trajectory interaction.

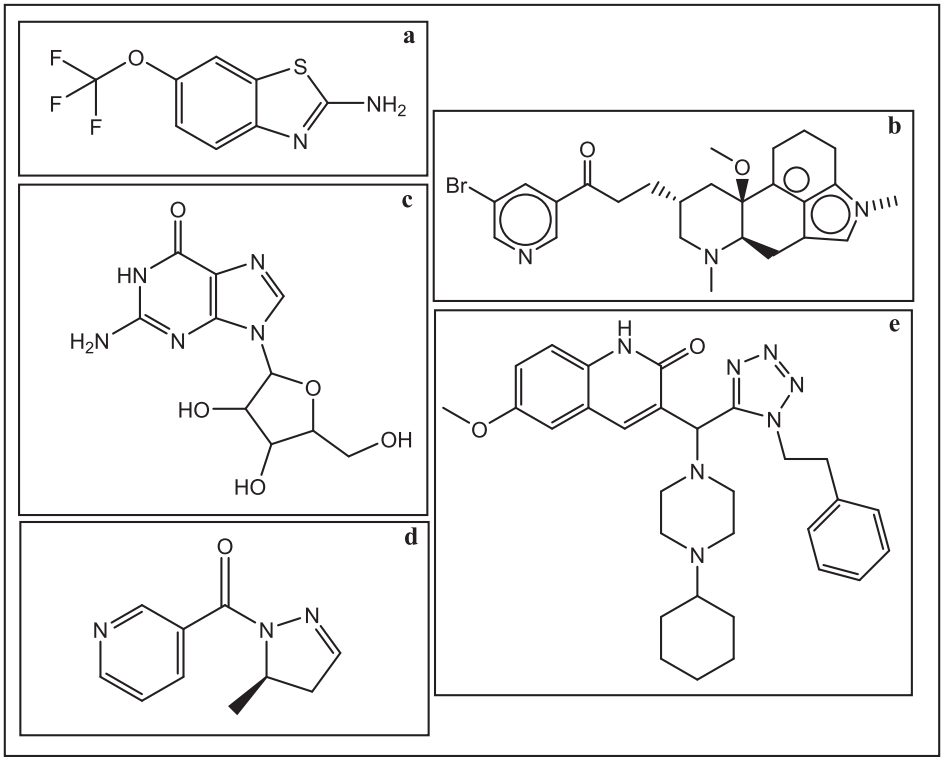

Fig. 6. Chemical structures of EAAT2 activators. **(a)** Riluzole, **(b**) Nicergoline, **(c)** Guanosine, **(d)** MS-153, and **(e)** GT949.

activator GT949 has a tetrazole moiety [30] (Fig. 6) are only a few examples of the existing specific activators that have been employed to activate EAAT2, but the use of these drugs has been limited due to their non-specific side effects, low bioavailability, and cardiac toxicity. The biological activity of a protein may be improved by the addition of substituted functional groups, electron-withdrawing groups, and electron-donating groups to 5-membered heterocyclic rings [45,46]. Therefore, a potential allosteric activator of EAAT2 is required for the early-occurring pathogenesis of AD to prevent Aβ-mediated oxidative damage and excitotoxicity. All these compounds exhibit the 5-membered heterocyclic ring; similarly, AK-968/15360623 also exhibits the 5-membered heterocyclic ring, which could be a potent molecule as compared to existing compounds in the treatment of AD.

Surprisingly, EAAT also functions as an anion channel. Heterologous expression studies revealed that EAAT1, EAAT2, and EAAT3 conduct a current carried by anions, independent of their glutamate transport activity. Until recently, this channel function was thought to be negligible and lacking any obvious physiological role. However, recent research has shown the physiological and pathophysiological roles of EAAT anion channels. EAAT2 anion channel hyperactivity has been implicated in cerebellar degeneration associated with episodic ataxia. The exact mechanism remains to be fully elucidated, but aberrant EAAT2 channel function could disrupt neuronal signaling and contribute to disease progression [47]. Similarly, in epileptic encephalopathy, EAAT2 anion channel dysfunction may play a key role. Elevated glutamate levels due to impaired EAAT2 function could lead to neuronal hyperexcitability and contribute to seizure activity [48].

Researchers have explored strategies to enhance EAAT2 expression as a potential therapeutic avenue. Small molecule activators of EAAT2 translation, such as LDN/OSU-0212320, have shown promise. LDN/OSU-0212320 protected neurons from glutamate-mediated excitotoxic injury and extended lifespan in an animal model of amyotrophic lateral sclerosis [49]. It also reduced mortality and neuronal death in a pilocarpine-induced temporal lobe epilepsy model [50]. While EAAT2 activators hold therapeutic potential, it's essential to recognize that their effects are multifaceted. The balance between glutamate transport and anion channel activity remains delicate. Allosteric activation of EAAT2 has the potential to impact both functions, necessitating thorough evaluation in future research to ensure therapeutic efficacy while minimizing risks to neurological health.

5. Conclusions

Our study focused on the identification of small-molecule allosteric activators targeting the EAAT2 protein, which plays a critical role in the uptake of glutamate and may have potential benefits for neurodegenerative diseases such as AD. Through virtual screening and molecular docking, we meticulously evaluated a vast synthetic compound database to prioritize potential candidates. In the current study, among the top-ranked compounds from HTVS, compound AK-968/15360623 emerged as the most promising allosteric activator based on its favorable binding characteristics and high affinity for allosteric binding site 1 of EAAT2. Additionally, compound AK-968/15360623 demonstrated excellent drug-like properties, including favorable lipophilicity, permeability across the blood–brain barrier, and a reduced risk of cardiac toxicity, making it a promising candidate for further development. The comprehensive analysis using MM-GBSA further confirmed the exceptional binding potency of compound AK-968/15360623, with a highly negative binding free energy value (−82.74 kcal/mol). Notably, this compound exhibited strong hydrophobic interactions, suggesting its ability to effectively interact with critical residues within the protein's binding pocket. Furthermore, the molecular dynamics simulation revealed the stability of compound AK-968/15360623 within the allosteric binding site of EAAT2, supporting its potential as an effective allosteric activator. The compound maintained its binding pose and exhibited satisfactory conformational stability throughout the simulation, enhancing its prospects for therapeutic application. Collectively, our study used *in-silico* methods to identify the allosteric activator AK-968/15360623 as a possible enhancer of glutamate uptake by EAAT-2. Therefore, this compound might possess the desired characteristics for

targeting neurodegenerative diseases with its ability to selectively activate EAAT2, that may facilitate the uptake of glutamate, and reduce oxidative stress and excitotoxicity. Our findings provide a solid foundation for further investigations, including preclinical and clinical studies, to explore the therapeutic potential of compound AK-968/15360623 and pave the way for the development of novel allosteric activators targeting EAAT2 in the treatment of AD and related neurodegenerative disorders.

CRediT authorship contribution statement

Chennu Manisha: Writing – original draft, Investigation. **Nagarjuna Palathoti:** Software, Formal analysis. **Jagdish Chand:** Writing – review & editing, Software. **Akey Krishna Swaroop:** Formal analysis. **Jubie Selvaraj:** Supervision. **B.R. Prashantha Kumar:** Software. **Prisil Naveentha X:** Visualization. **Brindha Durairaj:** Validation. **Antony Justin:** Supervision, Project administration.

Declaration of competing interest

The authors declare that they have no known competing financial interests or personal relationships that could have appeared to influence the work reported in this paper.

Acknowledgments

This study was supported by the Lady Tata Memorial Trust, Mumbai, India, for providing financial assistance for this research project. The authors also want to thank the Department of Science and Technology, Fund for Improvement of Science and Technology Infrastructure in Universities and Higher Educational Institutions (DST-FIST), New Delhi, India, for its contribution towards the development of the infrastructure of the Department of Pharmacology, JSS College of Pharmacy, Ooty, Tamil Nadu, India.

References

[1] N.C. Danbolt, Glutamate uptake, Prog. Neurobiol. 65 (2001) 1–105.
[2] R.J. Vandenberg, R.M. Ryan, Mechanisms of glutamate transport, Physiol. Rev. 93 (2013) 1621–1657.
[3] P. Beart, R. O'Shea, Transporters for L-glutamate: an update on their molecular pharmacology and pathological involvement, Br. J. Pharmacol. 150 (2007) 5–17.
[4] K. Kim, S.G. Lee, T.P. Kegelman, Z.Z. Su, S.K. Das, R. Dash, S. Dasgupta, P. M. Barral, M. Hedvat, P. Diaz, Role of excitatory amino acid transporter-2 (EAAT2) and glutamate in neurodegeneration: opportunities for developing novel therapeutics, J. Cell. Physiol. 226 (2011) 2484–2493.
[5] Y. Yatomi, R. Tanaka, H. Shimura, N. Miyamoto, K. Yamashiro, M. Takanashi, T. Urabe, N. Hattori, Chronic brain ischemia induces the expression of glial glutamate transporter EAAT2 in subcortical white matter, Neuroscience 244 (2013) 113–121.
[6] J. Lipski, C. Wan, J. Bai, R. Pi, D. Li, D. Donnelly, Neuroprotective potential of ceftriaxone in in vitro models of stroke, Neuroscience 146 (2007) 617–629.
[7] K. Chu, S.-T. Lee, D.-I. Sinn, S.-Y. Ko, E.-H. Kim, J.-M. Kim, S.-J. Kim, D.-K. Park, K.-H. Jung, E.-C. Song, S.K. Lee, M. Kim, J.-K. Roh, Pharmacological induction of ischemic tolerance by glutamate transporter-1 (EAAT2) upregulation, Stroke 38 (2007) 177–182.
[8] J.D. Rothstein, L.J. Martin, R.W. Kuncl, Decreased glutamate transport by the brain and spinal cord in amyotrophic lateral sclerosis, N. Engl. J. Med. 326 (1992) 1464–1468.
[9] J. Hardy, R. Cowburn, A. Barton, G. Reynolds, E. Lofdahl, A.-M. O'Carroll, P. Wester, B. Winblad, Region-specific loss of glutamate innervation in Alzheimer's disease, Neurosci. Lett. 73 (1987) 77–80.
[10] Braak H, Braak E. 1998. Evolution of neuronal changes in the course of Alzheimer's disease. ed.: Springer.
[11] P.T. Francis, Glutamatergic systems in Alzheimer's disease, Int. J. Geriatr. Psychiatry 18 (2003) S15–S21.
[12] C.M. Lauderback, J.M. Hackett, F.F. Huang, J.N. Keller, L.I. Szweda, W. R. Markesbery, D.A. Butterfield, The glial glutamate transporter, GLT-1, is oxidatively modified by 4-hydroxy-2-nonenal in the Alzheimer's disease brain: the role of Aβ1–42, J. Neurochem. 78 (2001) 413–416.
[13] R.L. Woltjer, K. Duerson, J.M. Fullmer, P. Mookherjee, A.M. Ryan, T.J. Montine, J. A. Kaye, J.F. Quinn, L. Silbert, D. Erten-Lyons, Aberrant detergent-insoluble excitatory amino acid transporter 2 accumulates in Alzheimer disease, J. Neuropathol. Exp. Neurol. 69 (2010) 667–676.
[14] H.A. Scott, F.M. Gebhardt, A.D. Mitrovic, R.J. Vandenberg, P.R. Dodd, Glutamate transporter variants reduce glutamate uptake in Alzheimer's disease, Neurobiol. Aging 32 (553) (2011) e551–e553, e511.
[15] D.J. Selkoe, Amyloid β-protein and the genetics of Alzheimer's disease, J. Biol. Chem. 271 (1996) 18295–18298.
[16] P. Mookherjee, P.S. Green, G. Watson, M.A. Marques, K. Tanaka, K.D. Meeker, J. S. Meabon, N. Li, P. Zhu, V.G. Olson, GLT-1 loss accelerates cognitive deficit onset in an Alzheimer's disease animal model, J. Alzheimers Dis. 26 (2011) 447–455.
[17] A. Schallier, I. Smolders, D. Van Dam, E. Loyens, P.P. De Deyn, A. Michotte, Y. Michotte, A. Massie, Region-and age-specific changes in glutamate transport in the AβPP23 mouse model for Alzheimer's disease, J. Alzheimers Dis. 24 (2011) 287–300.
[18] Fontana ACK, Guizzo R, Beleboni RdO, Meirelles e Silva AR, Coimbra NC, Amara SG, Santos WFd, Coutinho-Netto J. Purification of a neuroprotective component of Parawixia bistriata spider venom that enhances glutamate uptake. British journal of pharmacology 2003;139:1297-1309.
[19] A.C.K. Fontana, B.R. de Oliveira, M.W. Wojewodzic, W.F. Dos Santos, J. Coutinho-Netto, N.J. Grutle, S.D. Watts, N.C. Danbolt, S.G. Amara, Enhancing glutamate transport: mechanism of action of Parawixin1, a neuroprotective compound from Parawixia bistriata spider venom, Mol. Pharmacol. 72 (2007) 1228–1237.
[20] A.C. Pereira, J.D. Gray, J.F. Kogan, R.L. Davidson, T.G. Rubin, M. Okamoto, J. H. Morrison, B.S. McEwen, Age and Alzheimer's disease gene expression profiles reversed by the glutamate modulator riluzole, Mol. Psychiatry 22 (2017) 296–305.
[21] S.L. Lesuis, P.M. Kaplick, P.J. Lucassen, H.J. Krugers, Treatment with the glutamate modulator riluzole prevents early life stress-induced cognitive deficits and impairments in synaptic plasticity in APPswe/PS1dE9 mice, Neuropharmacology 150 (2019) 175–183.
[22] M.E. Frizzo, F.D. Schwalm, J.K. Frizzo, F.A. Soares, D.O. Souza, Guanosine enhances glutamate transport capacity in brain cortical slices, Cell. Mol. Neurobiol. 25 (2005) 913–921.
[23] M.E. Frizzo, D.R. Lara, K.C. Dahm, A.S. Prokopiuk, R.A. Swanson, D.O. Souza, Activation of glutamate uptake by guanosine in primary astrocyte cultures, Neuroreport 12 (2001) 879–881.
[24] M. Fioravanti, T. Nakashima, J. Xu, A. Garg, A systematic review and meta-analysis assessing adverse event profile and tolerability of nicergoline, BMJ Open 4 (2014) e005090.
[25] A. Nishida, H. Iwata, Y. Kudo, T. Kobayashi, Y. Matsuoka, Y. Kanai, H. Endou, Nicergoline enhances glutamate uptake via glutamate transporters in rat cortical synaptosomes, Biol. Pharm. Bull. 27 (2004) 817–820.
[26] F. Shimada, Y. Shiga, M. Morikawa, H. Kawazura, O. Morikawa, T. Matsuoka, T. Nishizaki, N. Saito, The neuroprotective agent MS-153 stimulates glutamate uptake, Eur. J. Pharmacol. 386 (1999) 263–270.
[27] A.C. Fontana, Current approaches to enhance glutamate transporter function and expression, J. Neurochem. 134 (2015) 982–1007.
[28] O.V. Mortensen, J.L. Liberato, J. Coutinho-Netto, W.F. Dos Santos, A.C. Fontana, Molecular determinants of transport stimulation of EAAT 2 are located at interface between the trimerization and substrate transport domains, J. Neurochem. 133 (2015) 199–210.
[29] S. Kortagere, O.V. Mortensen, J. Xia, W. Lester, Y. Fang, Y. Srikanth, J.M. Salvino, A.C. Fontana, Identification of novel allosteric modulators of glutamate transporter EAAT2, ACS Chem. Nerosci. 9 (2017) 522–534.
[30] R.M. Falcucci, R. Wertz, J.L. Green, O. Meucci, J. Salvino, A.C.K. Fontana, Novel positive allosteric modulators of glutamate transport have neuroprotective properties in an in vitro excitotoxic model, ACS Chem. Nerosci. 10 (2019) 3437–3453.
[31] D. Shivakumar, J. Williams, Y. Wu, W. Damm, J. Shelley, W. Sherman, Prediction of absolute solvation free energies using molecular dynamics free energy perturbation and the OPLS force field, J. Chem. Theory Comput. 6 (2010) 1509–1519.
[32] T. Kato, T. Kusakizako, C. Jin, X. Zhou, R. Ohgaki, L. Quan, M. Xu, S. Okuda, K. Kobayashi, K. Yamashita, Structural insights into inhibitory mechanism of human excitatory amino acid transporter EAAT2, Nat. Commun. 13 (2022) 4714.
[33] T.A. Halgren, Identifying and characterizing binding sites and assessing druggability, J. Chem. Inf. Model. 49 (2009) 377–389.
[34] T.A. Halgren, R.B. Murphy, R.A. Friesner, H.S. Beard, L.L. Frye, W.T. Pollard, J. L. Banks, Glide: a new approach for rapid, accurate docking and scoring. 2. Enrichment factors in database screening, J. Med. Chem. 47 (2004) 1750–1759.
[35] R.A. Friesner, J.L. Banks, R.B. Murphy, T.A. Halgren, J.J. Klicic, D.T. Mainz, M. P. Repasky, E.H. Knoll, M. Shelley, J.K. Perry, Glide: a new approach for rapid, accurate docking and scoring. 1. Method and assessment of docking accuracy, J. Med. Chem. 47 (2004) 1739–1749.
[36] E.M. Duffy, W.L. Jorgensen, Prediction of properties from simulations: free energies of solvation in hexadecane, octanol, and water, J. Am. Chem. Soc. 122 (2000) 2878–2888.
[37] C.A. Lipinski, F. Lombardo, B.W. Dominy, P.J. Feeney, Experimental and computational approaches to estimate solubility and permeability in drug discovery and development settings, Adv. Drug Deliv. Rev. 23 (1997) 3–25.
[38] C.R. Guimarães, M. Cardozo, MM-GB/SA rescoring of docking poses in structure-based lead optimization, J. Chem. Inf. Model. 48 (2008) 958–970.
[39] P.A. Kollman, I. Massova, C. Reyes, B. Kuhn, S. Huo, L. Chong, M. Lee, T. Lee, Y. Duan, W. Wang, Calculating structures and free energies of complex molecules: combining molecular mechanics and continuum models, Acc. Chem. Res. 33 (2000) 889–897.
[40] J. Li, R. Abel, K. Zhu, Y. Cao, S. Zhao, R.A. Friesner, The VSGB 2.0 model: a next generation energy model for high resolution protein structure modeling, Proteins Struct. Funct. Bioinf. 79 (2011) 2794–2812.

[41] Z. Guo, U. Mohanty, J. Noehre, T.K. Sawyer, W. Sherman, G. Krilov, Probing the α-helical structural stability of stapled p53 peptides: molecular dynamics simulations and analysis, Chem. Biol. Drug Des. 75 (2010) 348–359.
[42] W.L. Jorgensen, J. Chandrasekhar, J.D. Madura, R.W. Impey, M.L. Klein, Comparison of simple potential functions for simulating liquid water, J. Chem. Phys. 79 (1983) 926–935.
[43] M.A. Azam, A. Singh, Molecular insight into the binding mode of thieno [3, 2-c] pyrazol-3-ols with Streptococcus pneumoniae MurF enzyme by combined molecular modeling approach, Struct. Chem. 33 (2022) 491–503.
[44] N. Palathoti, K. Rajagopal, G. Byran, K. Raman, E. Jose, M. Gurunathan, Computational design for the development of natural molecules as compelling inhibitors against the target SARS-CoV-2: An in-silico attempt, Journal of Applied Pharmaceutical Science 13 (2023) 034–040.
[45] Jangir N, Poonam, Dhadda S, Jangid DK. Recent advances in the synthesis of five- and six-membered heterocycles as bioactive skeleton: A concise overview. ChemistrySelect 2022;7:e202103139.
[46] M. Hossain, A.K. Nanda, A review on heterocyclic: synthesis and their application in medicinal chemistry of imidazole moiety, Science 6 (2018) 83–94.
[47] Kovermann P, Untiet V, Kolobkova Y, Engels M, Baader S, Schilling K, Fahlke C. Increased glutamate transporter-associated anion currents cause glial apoptosis in episodic ataxia 6. Brain communications 2020;2:fcaa022.
[48] P. Kovermann, Y. Kolobkova, A. Franzen, C. Fahlke, Mutations associated with epileptic encephalopathy modify EAAT2 anion channel function, Epilepsia 63 (2022) 388–401.
[49] Q. Kong, L.-C. Chang, K. Takahashi, Q. Liu, D.A. Schulte, L. Lai, B. Ibabao, Y. Lin, N. Stouffer, C.D. Mukhopadhyay, Small-molecule activator of glutamate transporter EAAT2 translation provides neuroprotection, J. Clin. Invest. 124 (2014) 1255–1267.
[50] O.E. Zubareva, A.A. Kovalenko, S.V. Kalemenev, A.P. Schwarz, V.B. Karyakin, A. V. Zaitsev, Alterations in mRNA expression of glutamate receptor subunits and excitatory amino acid transporters following pilocarpine-induced seizures in rats, Neurosci. Lett. 686 (2018) 94–100.